Mem. S.A.It. Vol. 75, 458

Memorie della

XMM observations of three middle-aged pulsars

V. E. Zavlin[1] and G. G. Pavlov[2]

[1] Max-Planck Institut für extraterrestrische Physik, 85748 Garching, Germany
[2] Dept. of Astronomy and Astrophysics, Pennsylvania State University, 525 Davey Lab, University Park, PA 16802, USA

Abstract. X-ray observations of middle-aged pulsars allow one to study nonthermal radiation from pulsar magnetospheres and thermal radiation from neutron star (NS) surfaces. In particular, from the analysis of thermal radiation one can infer the surface temperatures and radii of NSs, which is important for investigating evolution of these objects and constraining the equation of state of the superdense matter in the NS interiors. Here we present results of *XMM* observations of three middle-aged pulsars, J0538+2817, B0656+14 and J0633+1746 (Geminga), and briefly discuss mechanisms of their X-ray emission.

Key words. stars: neutron – pulsars: J0538+2817, B0656+14, J0633+1746 (Geminga)

1. Introduction

A large number of isolated neutron stars (NSs) of various types, including active radio pulsars, have been observed with the currently operating large X-ray observatories, *Chandra* and *XMM*. Recent reviews on *Chandra* observations of NSs can be found in Pavlov et al. (2002); [PZS02] and Weisskopf (2002), while first *XMM* results are described by Becker & Aschenbach (2002). Here we discuss *XMM* observations of three pulsars, J0538+2817, B0656+14 (J0538 and B0656, hereafter) and J0633+1746 (Geminga), with ages of 30–300 kyr and spin-down energy loss rates of (3–5) $\times 10^{34}$ erg s^{-1} (see Table 1).

X-ray emission from an active pulsar generally consists of two components, thermal and nonthermal. In very young, bright pulsars ($\tau <$ 10 kyr) the thermal component is buried under the powerful nonthermal emission, while X-ray emission from old pulsars ($\tau \gtrsim 10^3$ kyr) is usually very faint. The intermediate group of middle-aged pulsars is particularly interesting for X-ray studies because they are expected to be bright and exhibit both thermal and nonthermal components. Below we present results of spectral and timing analysis of three middle-aged pulsars observed with the EPIC-pn instrument on board *XMM* .

2. PSR J0538+2817

This radio pulsar was observed with *XMM* in March 2002 (11.3 ks effective exposure for EPIC-pn, in small-window mode). The detected spectrum of J0538 can be fitted with a single blackbody model of $T_{\rm bb}^{\infty} \simeq 2.12$ MK, without invoking a nonthermal (power-law) component (McGowan et al. 2003). The blackbody model gives a small X-ray emitting area, with a radius $R_{\rm bb}^{\infty} \simeq 1.7$ km[1], much smaller than

Send offprint requests to: V. E. Zavlin
Correspondence to: zavlin@mpe.mpg.de

[1] All radii and luminosities are given for the distances listed in Table 1.

the expected NS radius ∼10 km. Such an area might be interpreted as a hot spot on the pulsar's surface. An alternative interpretation involves NS atmosphere models (see Zavlin & Pavlov (2002) [ZP02] for a review). A hydrogen atmosphere model with $B = 1 \times 10^{12}$ G fits the data even better (Fig. 1) and yields a lower (unredshifted) surface temperature $T_{\rm eff} \simeq 1.12$ MK and a radius $R \simeq 10.5$ km, consistent with the expected NS radius. An upper limit on the nonthermal X-ray luminosity in 0.1–10 keV is $L_X^{\rm nonth} < 1 \times 10^{31}$ erg s^{-1} $= 2 \times 10^{-4} \dot{E}$. Similar results were obtained by Romani & Ng (2003) from a *Chandra* observation, albeit with somewhat different model parameters (the discrepancy is probably due to a pile-up effect in the *Chandra* data). They also found an indication of a pulsar-wind nebula around J0538, with a size of $\sim 18''$, that cannot be resolved in the *XMM* data. However, the estimated luminosity of the nebula, $\sim 6 \times 10^{-5} \dot{E}$, is too low to seriously affect the analysis of the EPIC-pn data.

The EPIC-pn data also show pulsations of the X-ray flux, with one broad, asymmetric pulse per period (pulsed fraction $f_p \simeq 25\%$; McGowan et al. 2003). The phases of pulse maxima at energies below and above 0.8 keV differ by $\sim 75°$ (Fig. 2). Such pulsations show that the thermal emission is intrinsically anisotropic and indicate strong nonuniformity of the surface temperature and magnetic field.

3. PSR B0656+14

B0656 was observed with *XMM* in October 2001, with 6.0 ks and 25.0 ks EPIC-pn exposures in small-window and timing modes, respectively. The results of the spectral analysis of the EPIC-pn data are quite consistent with those derived from *Chandra* observations (PZS02). The X-ray spectrum shows at least two distinct components, thermal and nonthermal. The best fit is provided by a model consisting of soft (TS) and hard (TH) blackbody components, and a power law (PL; Fig. 3). The model parameters are $T^{\infty}_{\rm bb,s} \simeq 0.82$ MK, $R^{\infty}_{\rm bb,s} \simeq 7.3$ km (for TS), $T^{\infty}_{\rm bb,h} \simeq 1.72$ MK, $R^{\infty}_{\rm bb,h} \simeq 0.5$ km (for TH), and the photon index $\gamma \simeq 1.5$ (for PL). This model fits well the multiwavelength spectrum of B0656, from IR

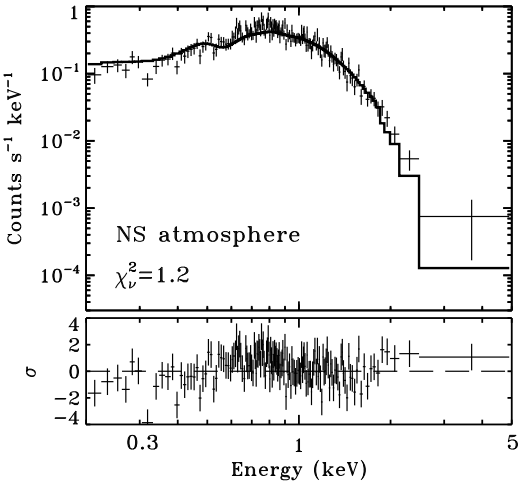

Fig. 1. EPIC-pn count rate spectrum of J0538 fitted with a magnetized hydrogen atmosphere model.

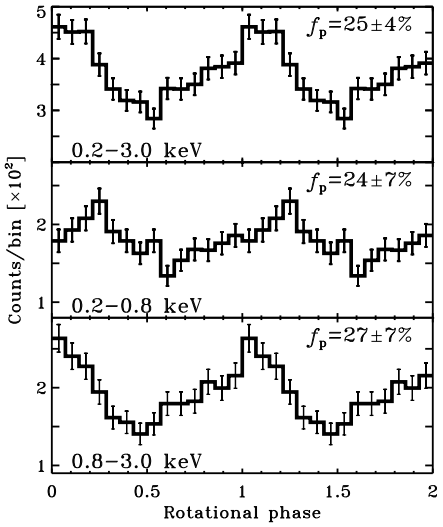

Fig. 2. X-ray light curves of J0538.

through X-ray energies (Fig. 4; see also PZS02 for details). However, even the larger radius, $R = [1 + z]^{-1} R^{\infty}_{\rm bb,s} \approx 5$–$6$ km (z is the gravitational redshift), is too small to be regarded as a NS radius. Using NS hydrogen atmosphere models for the thermal component yields distances $d \simeq 0.1$ kpc (at $R = 10$ km), a factor of three smaller than actually measured. The nonthermal component contributes only 1% of

Pulsar	P	τ	$\dot{E}$	B	d	F_X	L_X	$L_{\rm bol}$
	ms	kyr	10^{34} erg s^{-1}	10^{12} G	kpc	10^{-12} cgs	10^{32} erg s^{-1}	10^{32} erg s^{-1}
J0538	143	30	5	1	1.2	0.6	6.5	11.2
B0656	385	110	4	5	0.3	7.1	1.3	1.9
Geminga	237	340	3	2	0.2	1.8	0.2	0.5

Table 1. Pulsar parameters: period P, age τ ($P/2\dot{P}$ for B0656 and Geminga, and true age for J0538 — Kramer et al. 2003), rotational energy loss $\dot{E}$, surface magnetic field B, and distance d. Also, the energy flux F_X in 0.2–10 keV (as detected with EPIC-pn), the corresponding luminosity L_X (corrected for interstellar absorption) and the bolometric thermal luminosity $L_{\rm bol}$ are given.

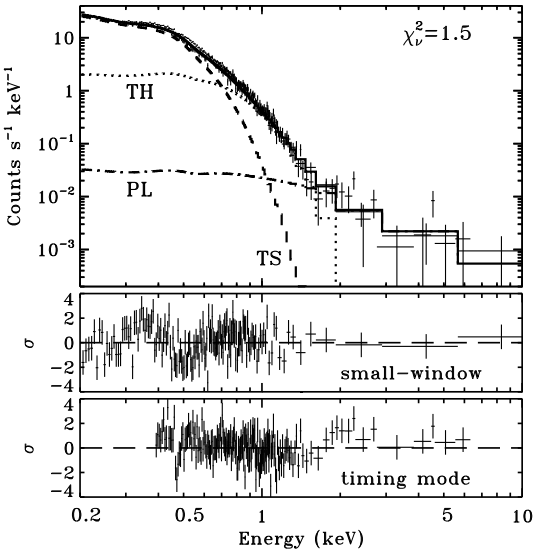

Fig. 3. EPIC-pn count rate spectrum of B0656 taken in two observational modes and fitted with a three-component model.

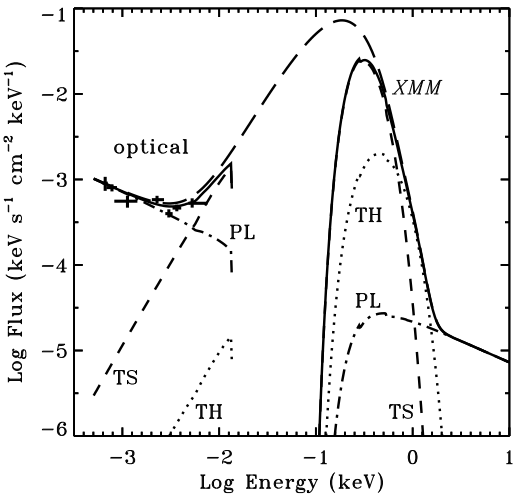

Fig. 4. Multiwavelength spectrum of B0656, with extrapolations of the total X-ray spectrum (long dashes) and its three components into the optical domain.

the total luminosity in 0.1–10 keV, $L_X^{\rm nonth} \simeq 2\times10^{30}$ erg s^{-1} $= 5\times10^{-5}\dot{E}$.

The timing analysis of the EPIC-pn data confirms that both the pulse shape and pulsed fraction strongly depend on photon energy (Fig. 5). The X-ray pulse profile of B0656 apparently consists of two components (centered at $\phi \simeq 0.6$ and 1.0), whose relative contributions depend on energy. The nonthermal emission at $E > 2$ keV shows one narrow peak per period, with $f_p \gtrsim 30\%$. Unfortunately, strong background contamination (especially in timing mode) prevents a more accurate analysis of pulsations at these energies.

4. Geminga

A long *XMM* observation of this famous γ-ray pulsar in April 2002 revealed a bow-shock nebula caused probably by the supersonic motion of the NS (Caraveo et al. 2003). The EPIC-pn effective exposure (small-window mode) was 71.4 ks. A large number of photons collected allows one to accurately measure the spectral parameters of the pulsar. The phase-integrated spectrum nicely fits a blackbody model, with $T_{\rm bb}^{\infty} \simeq 0.50$ MK and $R_{\rm bb}^{\infty} \simeq 10.6$ km, plus a power-law component with $\gamma \simeq 1.85$ (Fig. 6). Similar to B0656, the NS atmosphere models yield too large radius-to-distance ratios. The nonthermal component provides 7% of

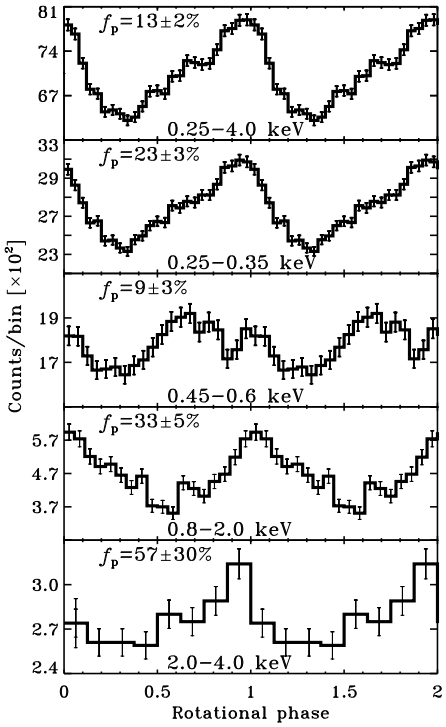

Fig. 5. X-ray light curves of B0656.

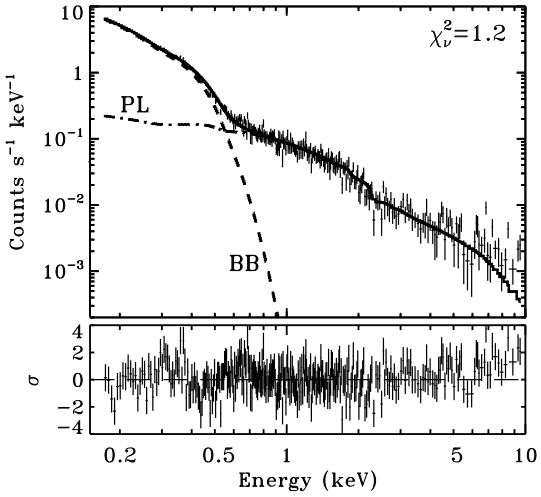

Fig. 6. EPIC-pn count rate spectrum of Geminga fitted with a two-component, blackbody (BB) plus power-law (PL), model.

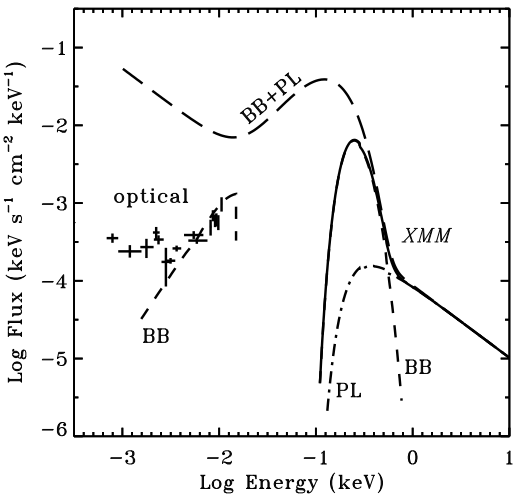

Fig. 7. Multiwavelength spectrum of Geminga, with extrapolations of the total X-ray spectrum (long dashes) and its thermal component into the optical domain.

the total luminosity in the 0.1–10 keV range[2], $L_X^{\rm nonth} \simeq 3\times10^{30}\,{\rm erg\,s^{-1}} \simeq 1\times10^{-4}\dot{E}$. The composite X-ray spectrum extrapolated into the optical domain (Fig. 7) exceeds the observed spectral fluxes by a factor of 50–100, whereas the extrapolated thermal component is close to the Rayleigh-Jeans spectrum observed in UV (Kargaltsev et al. 2004)

Similar to the case of B0656, the X-ray pulse profile shows a complex energy dependence (Fig. 8), with f_p growing up to almost 100% at $E > 2$ keV, where the emission is purely nonthermal. The shape of the light curve extracted in the 2–4 keV range is similar to that observed in gamma-rays, at $E > 100$ MeV (Mayer-Hasselwander et al. 1994).The two narrow peaks of the nonthermal emission are superimposed on the broad peak at lower energies. Phase-resolved spectroscopy shows that the photon index varies with phase from $\gamma = 1.7$ at $\phi \simeq 0.4$ (near the minimum of the composite light curve) to $\gamma = 2.0$ at the phase $\phi \simeq 0.7$ of the broader peak in the 2–4 keV range.

[2] The nebula might contribute a small fraction in the estimated nonthermal flux of the pulsar; a quantitative estimate is expected from a *Chandra* observation.

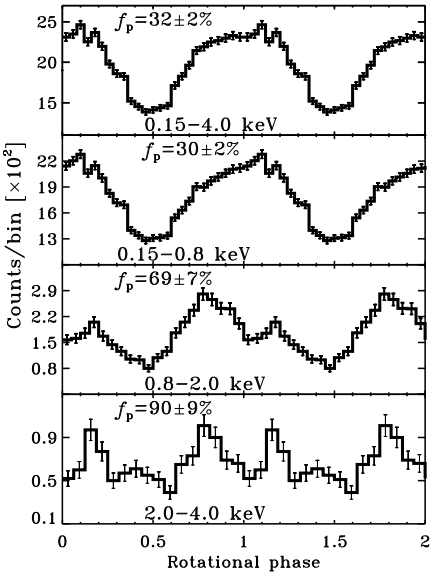

Fig. 8. X-ray light curves of Geminga.

5. Discussion

The main contribution to the X-ray fluxes of the three pulsars is provided by thermal emission from the their surfaces. The younger age of J0538 naturally explains its higher surface temperature, that is consistent with the standard NS cooling scenario. As discussed in ZP02, at such high temperatures ($\gtrsim 1$ MK) and relatively low magnetic fields, the NS surface is expected to be covered with a gaseous atmosphere, strongly ionized if comprised of hydrogen. Contrary to J0538, the older B0656 and Geminga are significantly colder and have stronger magnetic fileds. At such conditions, hydrogen atmospheres become denser and less ionized, and the currently available atmosphere models become less reliable. On the other hand, diffusive nuclear burning can reduce the hydrogen abundance in envelopes of cooling NSs (Chang & Bildsten 2003).In this case, the cooling hydrogen-depleted envelopes may undergo a phase transition, condensing into a liquid or solid surface. This may explain why the fits with hydrogen atmosphere models do not provide reasonable parameters for B0656 and Geminga, contrary to the younger and hotter J0538.

The observed temporal behavior of X-ray fluxes from these three pulsars indicates that their thermal radiation is locally anisotropic, in obvious contradiction with the simplistic blackbody interpretation of the phase-integrated spectra of B0656 and Geminga. Moreover, the asymmetry of the soft X-ray pulses (particularly for J0538 and B0656) hints that the surface distributions of temperature and magnetic field are not azimuthally symmetric, suggesting a strong multipolar component of the magnetic field or a decentered magnetic dipole. Whatever is the true nature of the complicated light curves, the NS parameters inferred from the blackbody spectral fits should be taken with caution. In particular, the comparison of the blackbody temperatures with the predictions of NS cooling theories may not be reliable, and the blackbody radii may be quite different from the actual NS radii.

The X-ray spectra of nonthermal emission from B0656 and Geminga are close to power laws, with a phase-dependent photon index in the latter case. While the power-law slopes and intensities (but not the light curves — Kern et al. (2003)) in the optical and X-ray bands are in agreement with each other for B0656, they strongly disagree for Geminga. It might be explained by the presence of two different populations of relativistic electrons in the pulsar's magnetosphere. The younger and more energetic J0538 shows no nonthermal X-ray radiation, in contradiction with a general expectation that younger pulsars with larger $\dot{E}$ are stronger nonthermal emitters. A simplest explanation of this contradiction is that the X-ray pulsar beam cannot be seen from the Earth. Alternatively, J0538 could be one of several pulsars with underluminous magnetospheric X-ray emission, — for instance, the famous Vela pulsar, whose age and thermal emission are similar to those of J0538, shows $L_X^{\rm nonth}/\dot{E} \sim 3\times10^{-6}$ (Pavlov et al. 2001), well below the upper limit of 2×10^{-4} inferred for J0538 from the *XMM* data.

Generally, the new observations confirm that middle-aged pulsars share a number of common features (in particular, pulsed thermal radiation), but their X-ray and, especially, multiwavelength emission properties are rather diverse. Thanks to the much improved quality of X-ray data, we are now quite certain that we do see the NS surface layers in soft X-rays, with temperatures $\lesssim 1$ MK, generally decreasing with NS age, and we do see strongly pulsed magnetospheric radiation at higher X-ray energies. On the other hand, we still do not completely understand the mechanisms of thermal emission (hence, cannot accurately measure the NS temperatures and radii, despite very small statistical errors), and we lack quantitative models for magnetospheric emission (hence, cannot infer the complex physics of NS magnetospheres from the measured phenomenological parameters). However, it is not surprising that we have not yet been able to solve all the puzzles from observations of a tiny fraction of these exotic (and diverse!) objects. The outstanding capabilities of the currently operating observatories, in both X-rays and optical, allow observations of a much larger sample of NSs, including thermally emitting midlle-aged pulsars, and we expect that our understanding of these elusive objects will be much better in a few years, provided enough observational time is allocated to NS studies.

Acknowledgements. Work of GGP was partly supported by NASA grant NAG5-10865.

References

Becker, W. & Aschenbach, B. 2002, in Proc. of the 270-th Heraeus Seminar on Neutron Stars, Pulsars and Supernova Remnants, eds. W. Becker, H. Lesch, J. Trümper, MPE Report 278, 64

Caraveo, P.A., et al. 2003, Science, 301, 1345

Chang, P. & Bildsten, L. 2003, ApJ, 585, 464

Kargaltsev, O., et al. 2004, in preparation

Kern, B., et al. 2003, ApJ, 597, 1049

Kramer, M., et al. 2003, ApJ, 593, L31

Mayer-Hasselwander, H.A., et al. 1994, A&A, 421, 276

McGowan, K.E., et al. 2003, ApJ, 591, 380

Pavlov, G.G., et al. 2001, ApJ, 552, L129

Pavlov, G.G., Zavlin, V.E. & Sanwal, D., 2002, in Proc. of the 270-th Heraeus Seminar on Neutron Stars, Pulsars and Supernova Remnants, eds. W. Becker, H. Lesch, J. Trümper, MPE Report 278, 273 (PZS02; `astro-ph/0206024`)

Romani, R.W. & Ng., C.-Y. 2003, ApJ, 585, L41

Weisskopf, M. 2002, in Proc. of the 270-th Heraeus Seminar on Neutron Stars, Pulsars and Supernova Remnants, eds. W. Becker, H. Lesch, J. Trümper, MPE Report 278, 58

Zavlin, V.E. & Pavlov, G.G. 2002, in Proc. of the 270-th Heraeus Seminar on Neutron Stars, Pulsars and Supernova Remnants, eds. W. Becker, H. Lesch, J. Trümper, MPE Report 278, 263 (ZP02; `astro-ph/0206025`)